 doi:10.20944/preprints201912.0279.v1

Article

On the Directivity of Lamb Waves Generated by Wedge PZT Actuator in Thin CFRP Panel

Sergey Shevtsov [1,*], Valery Chebanenko [2], Maria Shevtsova [3], Shun-Hsyung Chang [4], Evgenia Kirillova [5] and Evgeny Rozhkov [6]

[1] FRC The Southern Scientific Centre of Russian Academy of Science; sergnshevtsov@gmail.com
[2] FRC The Southern Scientific Centre of Russian Academy of Science; valera@chebanenko.ru
[3] FRC The Southern Scientific Centre of Russian Academy of Science; mariamarcs@bk.ru
[4] National Kaohsiung University of Science and Technology; stephenshchang@me.com
[5] RheinMain University of Applied Science; evgenia.kirillova@hs-rm.de
[6] Southern Federal University; rozhkov@math.rsu.ru
* Correspondence: sergnshevtsov@gmail.com; Tel.: +7-903-401-3385

Abstract: This paper addresses investigation of guided-wave excitation by angle-beam wedge piezoelectric transducers in multi-layered composite plate structure with orthotropic symmetry of the material. The aim of present study is to determine the capability of such actuators to provide the controlled generation of acoustic wave of desirable type with the necessary wavelength, propagation distance and directivity. The studied CFRP panel is considered as homogenous with effective elastic moduli and anisotropic structural damping, whose parameters were determined experimentally. According to the results of dispersion analysis and taking into account the data of wave attenuation in a highly damping CFRP composite, two types of propagating waves A0 and S0 were considered theoretically and experimentally in the frequency range 10 - 100 kHz. Using the results of a previous study, the structure of the wedge actuator was reconstructed to develop its finite element (FE) model, and a modal analysis was carried out, which revealed the most intense natural vibration modes and their eigenfrequencies within the used frequency range. Both experimental and numerical studies of the generation, propagation, directivity and attenuation of waves in the orthotropic composite panel under study revealed the influence of the angular orientation of the actuator on the formation of wave patterns and allowed to determine the capabilities of the wave's directivity control.

Keywords: : acoustic based SHM; orthotropic polymeric composites; Lamb waves; horizontally polarized SH waves; angle-beam wedge transducer; waves directivity

1. Introduction

A wide spread of the glass-fiber (GFRP) and carbon-fiber reinforced polymeric composites in aircraft, automotive and shipbuilding industries require a reliable, cost-effective and easy to use means for the Structural Health Monitoring (SHM) and Nondestructive Evaluation (NDE) to supply the quality and defect-free products. Such methods and the necessary tools are most in demand in manufacturing of load carrying structures, whose defects can cause emergencies or some dangerous failures. Among the known SHM and NDE methods of the polymeric composite materials the acoustic based methods are most effective and used in practice [1 - 4]. The common difficulties at the design of efficient acoustic based SHM of polymeric composites are the structural anisotropy of the elastic [2] and high damping properties [1, 5 - 9] of the materials that reduces the wave propagation distance [9, 10]. The carbon fiber reinforced composite materials present additional challenges for inspection due to their conductivity of the fibers, the insulating properties of the matrix, and the fact that damage often occurs beneath the visible surface [2]. Meanwhile, the collective skills of many researcher confirm that in some cases Lamb wave based SHM techniques can provide more reliable

information about damage presence and severity than another methods, and provide the possibility of determining damage location due to their local response nature. These imperfections that can be detected by the acoustic SHM are delaminations, inclusions, uneven resin cure areas and porosity [11], the dry spots, which can arise during liquid composite molding [12, 13] and even the errors of lay-up stacking orientation [14].

In order to detect, identify the geometric location and severity of the probable imperfection the proper choice of the wave type, length and intensity within the whole scanned area should be surely fulfilled , that is the first task of each acoustic-based SHM technique. This choice should provide the necessary resolution, wave propagation distance and directivity, which depend on the composite's elastic and damping properties anisotropy, on the excited wave type and frequency.

An influence of the structural anisotropy of the material on the wave propagation in the plate-like composite structures has been studied in many works. The one of the early works reported to the sufficient influence of structural anisotropy on the acoustic waves propagation was the paper [17], where both static and dynamic values of the storage moduli of the laminated beams were predicted from unidirectionally reinforced ply data, and their values were used to predict the wavespeeds in two quasi-isotropic laminates. The article [16] notes that there is little or no theoretical basis, which is provided by researchers for the optimal choice of the various testing parameters involved such as transducer geometry, dimensions, location and materials, excitation frequency, bandwidth, especially, for the anisotropic tested material. The authors proposed the new approach, which is based on the assembling the laminate global matrix from the individual layer matrices, yields traveling waves along both directions in the plane of the plate. The developed approach was applied to two quasi-isotropic symmetric laminates with different lay-ups. The quasi-isotropic laminates were studied experimentally in [14] for the detection lay-up stacking orientation. The paper [8], which experimentally studied the Lamb waves attenuation in the quasi-isotropic plastic, demonstrates a sufficient decrease of the propagating wave amplitude with angle between main axis of anisotropy and wave path. Hu with coworkers [11] investigated the A0 and S0 waves propagation and their sensitivity to the delamination in cross-ply laminates. It should be noted that all of the above works [2, 8, 11, 14], as well as other articles [16 - 18] that investigated the influence of the anisotropy of the elastic properties of the material on the propagation of acoustic waves, tested the proposed models and calculation methods on quasi-isotropic and cross-ply laminates.

The distance of the wave propagation the authors of [9, 10] divides onto four phenomena:

- Geometric spreading;
- Material damping;
- Wave dispersion;
- Dissipation into adjacent media.

An attenuation of a circular wave propagating in a damped plate is described by the relation

$$\phi(r,t) = \left(A/\sqrt{r}\right)\cdot e^{-\eta r} e^{i(\omega t-\gamma r)}, \quad (1)$$

where r is the distance between the wave source and the amplitude measuring point, A is the magnitude of the signal, $\phi(r, t)$ is a generic disturbance that propagates in space as a wave, γ is the wave number, ω is the angular frequency, and η is the wave damping coefficient, which depends on following phenomena [10, 22]:

- Viscoelastic nature of matrix and/or fiber materials;
- Damping due to interphase interaction;
- Damping due to damage;
- Viscoplastic damping due to the presence of high stress and strain concentration that exists in local regions between fibers;
- Thermo-elastic damping due to cyclic heat flow from the region of compressive stress to the region of tensile stress.

This list make it obvious the damping's anisotropy of the multilayered composites with differently oriented layers.

 doi:10.20944/preprints201912.0279.v1

The propagation of attenuating waves generated by the omnidirectional circular PZT actuators in a CFRP plate with significant anisotropy of elastic and dissipative properties was studied in the authors' works [19, 20], where the properties of an orthotropic material were previously determined as effective modules in accordance with the methodology considered in [21].

In the early study [23] it was established that fibers material usually have extremely low damping capacities and so can be considered not to contribute to the damping of the composite, whereas a large proportion of the dissipated energy must be in the matrix. The higher damping capacity of the composite under torsion than flexure may be attributed to the higher distortional energy induced in the matrix since very little (if any) energy is dissipated as a result of dilatational strains, and the higher potential for interfacial slipping of the torsion case.

The work [24] reported about many experiments implemented with different kinds of CFRP and GFRP laminas demonstrated a significant growth of the damping parameters (up to ten times and more) with change the cyclic strain orientation relative to the fibers direction. Moreover, these damping parameters are frequency dependent, and they always increase with the frequency, especially, for the cyclic strain normal to the fibers direction. This work confirms experimentally validity of the Hashin equation [25], which describes the dependence of the flexural loss factor η on the fiber volume fraction in composites

$$\eta = \eta_m \Big/ \left[1 + \frac{E_f V_f}{E_m \left(1 - V_f\right)} \right] \tag{2}$$

where η_m is the loss factor of the matrix, E_f and E_m, are the real parts of the complex modulus of the fiber and resin respectively and V_f is the fiber volume fraction. The theoretical approach for determination of the frequency dependent loss factor of the laminated composites, which are proposed in this report, is based on the similar dependencies of the lamina's loss factors at the longitudinal, transversal and shear cyclic strains, and on the classical lamination theory relations [26].

The basic elasticity relationships for unidirectional composites, together with the Adams-Bacon damping criterion, are utilized in [27] for prediction of moduli and flexural damping of anisotropic CFRP and GFRP beams with respect to fibre orientation. This criterion postulates that the energy dissipation in a thin unidirectional lamina is the sum of separable energy dissipations due to σ_x, σ_y, and τ_{xy}. The proposed approach was used to obtain the variation of elastic moduli and the damping capacities of the beams with different angle-ply orientation. The calculation results, which were confirmed experimentally, revealed very intensive angular dependencies of the damping parameters for the orthotropic composites. Moreover, the structural damping increases with increasing of deviation angle from the main axis of anisotropy.

Validity of these conclusions were confirmed in the article [18], which contains the results obtained at the experimental study of the wave attenuation along and across unidirectional CFRP, cross-ply and quasi-isotropic composites for the different kinds of acoustic waves propagation at the varied frequencies. The similar results are presented in the later paper [22], where the dynamic characteristics and vibration damping properties of fiber-reinforced, polymer-matrix composites, with emphasis on parameters governing damping, such as fiber volume fraction, fiber orientation, exciting frequency, aspect ratio and fiber-matrix interface, as well as stacking sequence for laminated composites are considered.

In order to estimate the wave propagation distance at the implementation of the acoustic-based SHM systems for the cross-ply and quasi-isotropic composites, the analogous studies were carried out and whose results are presented in the works [5] and [8]. The present results demonstrate a sufficient decrease of the propagating Lamb wave amplitude with angle between main axis of anisotropy and wave path. It was established also than attenuation of the flexural A0 mode is much higher than the extensional S0 mode. Another important result reveals that quasi-isotropic $[0,45,-45,90]_{2s}$ plates are useful in design, but stress wave inspection is difficult due to high attenuation of both Lamb modes. It's obvious, this conclusion relate to all CFRP and GFRP plates with complex lay-up and anisotropy. The authors of the paper [8] concluded that it is necessary to accumulate more experimental results before consistent phenomena interpretations can be

developed. However, understanding these characteristics will benefit future acoustic based SHM and NDE applications in composite materials design and technology.

The difficulties of the reliable estimation of the waves attenuation in the multilayered composites by using the experimental data of the lamina damping properties, their dependence on the fiber volume fraction, frequency, strains type and amplitude, which are included into some model of the wave attenuation, led to development the experimental technique [9] for determine the attenuation properties directly at the study of the excited waves propagation. The comparative analysis of the relation (1) with the experimental results, which were performed in [9], demonstrated that reduction in amplitude of a Lamb wave is very steep nearer to the excitation source, and this reduction in amplitude is independent of the material attenuation. When moved away from the source, the reduction in amplitude is due to both geometry and material damping, but latter dominates. The proposed technique we used in our previous work [19] to determine experimentally the angular distribution of attenuation coefficient for the studied orthotropic laminate. These results we use in the present paper.

It seems important to compare the excitation frequencies of Lamb waves used by various authors for the purpose of their use in SHM systems designed to acoustic scanning of multilayered fiber reinforced polymeric composites. Schultz and Tsai [17] reported that they were able to reliably measure the wave attenuation in the laminated beams at the frequencies no more than 10 kHz. Later studies using modern advanced equipment were able to operate at higher frequencies. The results of the acoustic based damage detection present in [1] were obtained at the relatively low excitation frequency, in the range 15-50 kHz that is due to very high Lamb waves attenuation in the studied composite panels. The work described in [11], which compared the sensitivity of A0 and S0 Lamb wave to the delamination in CFRP cross-ply laminated beams, established that due to the very intensive Lamb wave attenuation two excitation frequencies: 45 and 80 KHz were used to diagnosis the delaminations with length 8 - 30 mm. The authors of this paper securely recorded an attenuation of the Lamb waves excited by the circumferential PZT actuators in the orthotropic CFRP panel using frequencies within the range 10 - 100 kHz [20]. Apparently, the boundaries of this range determine the frequencies at which it is possible to provide a sufficient propagation distance for traveling Lamb waves.

The fact that the attenuation of waves in anisotropic materials is also anisotropic makes us pay special attention to the possibility of controlling the directivity of the generated waves. The abilities of the sources of acoustic waves, including their frequency ranges, intensity, directivity, is given in the comprehensive review paper [3]. Raghavan and Cesnik in their paper [16] noted that there is little or no theoretical basis, which is provided by researchers for the optimal choice of the various testing parameters involved such as transducer geometry, dimensions, location and materials, excitation frequency, bandwidth, especially, for the anisotropic tested material. Using a modified semi-analytical approach based on the spatial Fourier inversion and the simplest delta-like and Heaviside forcing functions due to piezoelectric actuators of circular, ring-shaped and rectangular shapes, which act on the plate surface by the shear stress, and neglecting by their enough complex, frequency dependent distribution on interface, they determined the dependence of generated Lamb waves on the actuators' properties. The developed approach was successfully applied to two quasi-isotropic symmetric laminates with different lay-ups. Such approach, which can be used for the omnidirectional transducer with sufficient simplification of their forcing functions, has been used by many researchers. Its advantages and limitations were analyzed in the experimental work [28], which used a scanning laser Doppler vibrometer (SLDV) as a receiver with the ability of the spatially dense sensing, allowing to analyze of the wave propagating at the different angles from the omnidirectional wave exciter. Ostiguy with co-workers argued in the paper [29] that at the analytical modeling of guided waves generation by a circular PZT and propagation the analytical formulations need to consider (1) the dependency of phase velocity and damping as a function of angle, (2) the steering effect on guided wave propagation caused by the anisotropy of the structure, and (3) the full transducer dynamics. The most important feature of the performed study was dynamic analysis of the system "circular PZT actuator-composite panel" that allowed to reveal the in-plane stress

 doi:10.20944/preprints201912.0279.v1

distribution on interface and obtain the qualitative estimation of the influence of the anisotropic damping on the wave attenuation. The radial shear stress calculated at specific frequencies shows that the in-plane shear stress (1) vary in amplitude over the frequency range of interest; (2) are dependent on the orientation, and (3) are not only located at the edge of the PZT. The finite element implementation of the similar approach was applied by the authors of the present paper at the study of the directivity of Lamb waves generated by the circular PZT actuators of different dimensions at the varied excitation frequency [20]. In the reviewed works an important limitation inherent to omnidirectional actuators has been revealed. This limitation is an impossibility to controllable change of their directivity. To overcome it the following approaches has been developed applying to the problem of controlled directivity of the excited guided waves: use of distributed PZT transducers array, which generate selectively the desirable Lamb modes [30]; active fiber composites and macro-fiber composites due to their broad frequency of operation, high reliability and easy installation [6, 15]; interdigital transducers, which able to generate bidirectional waves with relatively low side lobe level [6]. However, SHM of the large composite structures, where acoustic waves generated by the spatially fixed exciter quickly attenuate and cannot spread over long distance, is difficult. This makes it necessary to use actuators that make it easy to change their location and angular orientation on the test structure that is very important for the anisotropic materials.

Among many modern and widespread design of the transducer for the acoustic waves generation the angle-beam wedge transducers, which are traditionally used for the SHM of thick walled structures made of isotropic metallic materials, are considered in the survey [3]. The first fundamental study of the wedge transducers were presented in monograph [31], where the conditions for the optimal transformation of the longitudinal waves generated by the PZT plate to the surface Rayleigh wave in the tested structure.

Some modernizations of the wedge actuators to eliminate the reflections at the wedge-load interface and multiple reflections inside the wedge were described in [33, 33].]. It has been shown in [34] that the width of the so-called "phase velocity spectrum" is dependent only upon the ratio of loading length to wavelength of the mode being generated. In the work [34] was assumed that the transducer produces a very simplified roughly parabolic pressure distribution

$$p(\alpha)=\begin{cases}\sigma_0\left(1-\dfrac{\alpha^2}{(D/2)^2}\right) & if \quad |\alpha|\le D/2\\ 0 \quad if \quad |\alpha|>D/2\end{cases} \tag{3}$$

where σ_0 represents the maximum pressure which occurs at the center of the transducer face, $(\alpha=0)$, and the transducer has a width D. It was proven that for a given frequency, there will be a finite number of real wavenumbers (that can be excited), satisfying the dispersion equation at the general case of anisotropic tested material.

The paper [35] studied the effect of dimensions, shape and aperture on frequency response and directivity of the waves generated by the angle-beam wedge transducer in a isotropic half space using the boundary element method. The authors note the main disadvantages of a large transducer due to so named aperture effects. These include signal distortion, the fact that certain frequency components may be cut off, and the near field effect. The authors present the results of a comprehensive parametric study in an effort to establish guidelines and criteria for optimum wedge transducer design. The main objective of the study is the optimal choice of the wedge shape and dimensions to avoid spurious eigenmodes or unexpected wave propagations within the wedge. The main conclusions include some recommendation about dependence of the trapezoidal wedge quality criteria on the contact area, height of transducer and its angles, which can be used in the design of the SHM system for the specific material and tested structure. In the paper [36], which study the similar problems, the effect of the shape and size of wedge-shaped substrates on the whole transducer system is discussed, and the design of a transducer is optimized to supply its performance when generates the acoustic wave in a tested thick-walled structure made of isotropic material with the specific acoustic impedance by using a 2D Finite Element (FE) model.

 doi:10.20944/preprints201912.0279.v1

The later studies of the wedge actuators excited the acoustic waves in an isotropic elastic half-space by using more sophisticated three-dimensional (3D) models that rely on highly numerical approaches such as finite elements, boundary elements, multi-Gaussian beam (MGB) or the distributed point source (PSM) methods [37 - 40].

To find out the possibility of generating directed acoustic waves in thin-walled structures using a wedge actuator, the authors of the current article investigated this problem by reconstructing the dynamics of the entire system, including the structure of the actuator and the quasi-isotropic plastic plate under test. To do this, 3D coupled transient problem of piezoelectricity and mechanics for a system of bodies made of elastic materials having different structural damping was formulated and solved by the finite element method. The results of our numerical investigations, which were confirmed experimentally, revealed that upper limit of the excited frequency range is determined by the damping of the material of structure under testing. The highest efficiency, intensity and propagation distance of the waves generated by the wedge actuator are achieved when the waves are excited at the eigenfrequencies of its natural vibration modes. The directivity of the propagated waves depends on the shear stresses distribution on the actuator-panel interface, i.e. on the selected actuator's oscillation mode. The directivity of the propagated waves depends on the shear stresses distribution on the actuator-panel interface, i.e. on the selected actuator's oscillation mode.

This paper is aimed to reveal the possibility of generating directed acoustic waves by the angle-beam wedge actuator in thin-walled structures made of highly anisotropic material. As objects of our study we used the orthotropic CFRP panel and angle-beam wedge actuator Olympus V414-SB-ABWS, which was modeled and experimentally investigated in our works [19, 20]. By using experimentally verified frequency response functions for the displacement amplitudes and the electric current consumption of the actuator the testing frequencies were selected. The directivity of the excited anti-symmetric A0 Lamb wave was studied at the different orientation of actuator relative to the main axis of orthotropic material. These directivity diagrams are present at the end of this paper together with the radial shear stress distribution on interface to demonstrate their interdependence. All obtained results and developed technique are intended to clarify the abilities of the angle-beam wedge actuator at its use for SHM of orthotropic composite materials.

2. Materials and Methods

Our investigation includes three stages, and besides, each stage was performed both experimentally and theoretically. First, we determine the dispersion relations to find the kinds and wavelengths of the acoustic waves that can be excited in the studied composite structure. In order to solve the dispersion equations all mechanical properties for the studied composite panel made of orthotropic CFRP are adopted from our early research, whose results were published in [19, 20], wherein the frequency range for excited wave was chosen taking into account the waves attenuation data from these papers.

To simulate the wave propagation in the studied CFRP panel the numerical finite-element (FE) model of the used wedge transducer was identified on the base of the results of its experimental investigation, which provided data on the dynamic properties of the actuator required to develop an adequate device's model.

The full-scale experiment and FE simulation of the acoustic waves propagation in the orthotropic panel were implemented at the chosen excitation frequencies and variation of the wedge actuator orientation relative to the main axis of orthotropic material of CFRP panel. The results of these studies are presented in the form of the waves directivity diagrams and angular dependencies of the propagated waves attenuation. The obtained results are matched with the distributions of the stresses and displacements on the interface between actuator's footprint and surface of the tested panel to understand the ability of the wedge transducer to generate the spatially oriented wave beams.

Preprints (www.preprints.org) | NOT PEER-REVIEWED | Posted: 21 December 2019 doi:10.20944/preprints201912.0279.v1

2.1. Dispersion analysis of the waves that can be excited in CFRP panel under study

The investigated CFRP panel was manufactured by the laying-up of unidirectional carbon-fiber epoxy based prepreg according to scheme $[0^0;-30^0;30^0;90^0]_{2s}$ to produce a symmetric balanced laminate. Its elastic properties were determined by two independent methods. The longitudinal E_1, transversal E_2, in-plane shear G_{12} moduli and Poisson ratio ν_{12} were calculated using prepreg's manufacturer data of lamina elastic properties and relations of the classical lamination theory [26]. The experimental technique included determination of these moduli experimentally according to ASTM standards and a refinement technique to reduce the effect of non-ideal experimental conditions [21]. Through thickness module E_3, interlaminar shear moduli G_{23}, G_{31} and Poisson ratios ν_{23}, ν_{31}, unavailable for reliable experimental measurement, were calculated using FE simulation of the static tests for the multilayered composite [42]. The confidence intervals for all elastic constants were calculated using the experimentally measured ones, obtained for every 5 tested specimens. The final results of the elastic moduli of the studied CFRP panel, which are presented in Table 1, are typical for an orthotropic structural symmetry of composites.

Table 1. The calculated elastic moduli of CFRP panel [1].

Young's moduli, GPa			**Shear moduli, GPa**			**Poisson's ratios**		
E_1	E_2	E_3	G_{12}	G_{23}	G_{31}	ν_{12}	ν_{23}	ν_{31}
63±12	22.5±2.5	5±1.5	9.6±1.2	7.3±0.6	7.8±0.6	0.46±0.06	0.32±0.08	0.6±0.1

[1] The bounds of the confidence intervals for the elastic moduli are determined using measuring data.

The dispersion analysis of acoustic waves phenomena in the studied CFRP panel was performed only for the longitudinal (x_1) and transversal (x_2) directions of the CFRP orthotropic coordinate systems. The dispersion curves were calculated by numerically solving the equations (4, a) for the symmetric and (4, b) for the anti-symmetric Lamb wave modes [43] within the frequency range (10 - 100 kHz) that is due to intensive waves attenuation at higher frequencies.

$$\left(q^2-k^2\right)^2\cdot\sin(qh)\cdot\cos(ph)+4k^2pq\cdot\sin(ph)\cdot\cos(qh)=0 \qquad (4,\text{ a})$$

$$\left(q^2-k^2\right)^2\cdot\sin(ph)\cdot\cos(qh)+4k^2pq\cdot\sin(qh)\cdot\cos(ph)=0 \qquad (4,\text{ b})$$

Equations (4, a, b) include the following quantities: $p^2=\omega^2/c_L^2-k^2$; $q^2=\omega^2/c_T^2-k^2$, where $k=\omega/c$ is the wavenumber, ω is the angular frequency, $c_L^2=(\lambda+\mu)/\rho$ and $c_T^2=\mu/\rho$ are the pressure and shear wave speeds, respectively, λ and μ are the Lame constants, h is the half-thickness of the flat CFRP panel, and ϱ is the material's mass density. In order to determine the bounds of the possible variation of the wavespeeds and wavelengths due to limited measurement accuracy of elastic modules these equations were solved using the upper and lower values of moduli (see Table 1). The measurement of the wavespeeds was performed using wave's "time of flight" between sensors, which were placed along the wave paths. Their mean values are denoted by the point markers in Figs. 1 and Fig. 2.

Dispersion of the horizontally polarized shear waves was analyzed by solving the equation (5), which has only one symmetric solution within the studied frequency range [43].

$$4k^2h^2\left[(c/c_T)^2-1\right]/\pi^2=n^2;\quad n=0,1,... \qquad (5)$$

As within the frequency range (10 - 100 kHz) this equation for both propagation directions (x_1 and x_2) has only one zero-order solution corresponding to n=0, the symmetric SS0 waves propagate with the changeless speeds $c=c_T$. The dispersion of its wavelengths is present in Figure 2.

Comparison of Fig. 1,b with Fig. 2 demonstrates that wavelength of A0 Lamb waves mode is 2 - 5 time less than wavelength of SS0 horizontally polarized shear wave, i.e. spatial defects resolution of A- waves can be significantly better that is fully consistent with the results of the papers [11, 20, 22, 30].

Preprints (www.preprints.org) | NOT PEER-REVIEWED | Posted: 21 December 2019 doi:10.20944/preprints201912.0279.v1

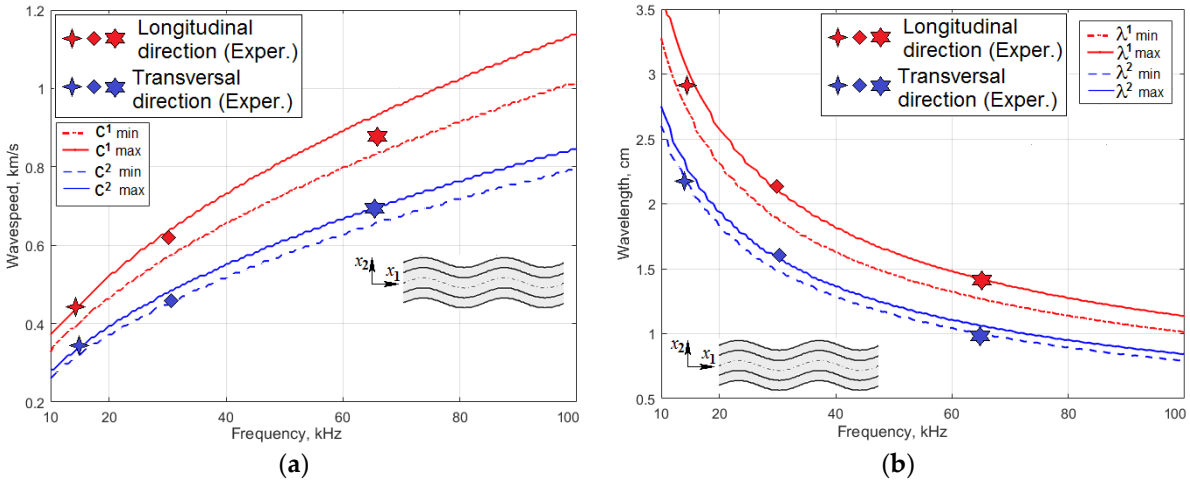

Figure 1. The dispersion curves for the anti-symmetric A0 Lamb waves propagating along (¹) and across (²) the main axis of orthotropic symmetry

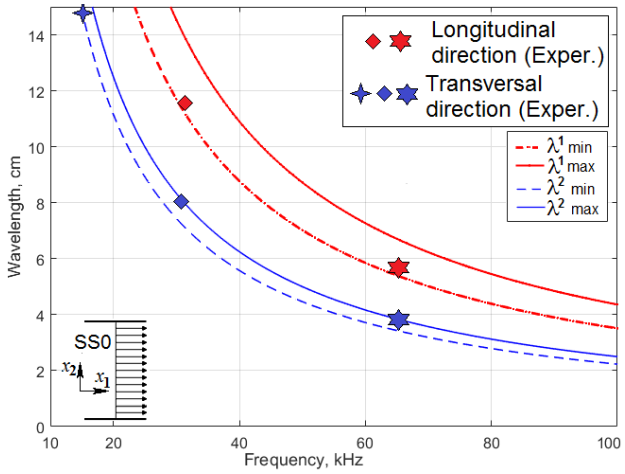

Figure 2. The dispersion curves for the symmetric horizontally polarized shear waves SS0 propagating along (¹) and across (²) the main axis of orthotropic symmetry

2.2. The finite-element model of the angle-beam wedge actuator, generating the wave in a thin CFRP panel

The second important component of the studied system is the angle-beam wedge actuator, which excites the acoustic waves in the CFRP panel under consideration. In order to develop the finite-element model of the full system's dynamics that should be quantitatively comparable with the response of a real-world experimental system, the electrical and mechanical subsystems properties of the modeled actuator need to be as close as possible to the properties of the used Olympus actuator. Identification technique of its structure and electro-mechanical properties was presented in our paper [41]. The sources, which have been used to adequately build the transducer's structure and replicate its dynamics in FE model, are the technical notes about the ultrasonic principles important to wedge transducer application and design, including scheme and main requirements to the active element, backing, matching layers and the soundpath presented by Olympus Co.® [44], the outer dimensions of the used actuator (see Fig. 3), the frequency response functions for the electric current through PZT active plate, and out-of-plane displacement amplitude on the actuator's footprint (see Fig. 4, a, b), which have been determined experimentally. Only averaged normal displacements of the actuator's contact surface were measured experimentally by using the calibrated sensors, which are sensitive to the normal acceleration. The displacement amplitudes were calculated after double integration the sensor's signal over time for each frequency. In order to compare the experimental and simulation results the displacements of the modeled actuator contact surface were averaged within the footprint. The tangent displacement cannot be

Preprints (www.preprints.org) | NOT PEER-REVIEWED | Posted: 21 December 2019 doi:10.20944/preprints201912.0279.v1

measured experimentally by the available means. They are present as the results of computer simulations of the actuator's FE model, whose geometry is present in Figure 5. This model was implemented in the Comsol Multiphysics FE tool, which allow to easy tune elastic, damping properties of each actuator's component and to orient the polarization direction of the active PZT plate along the soundpath made of Lucite.

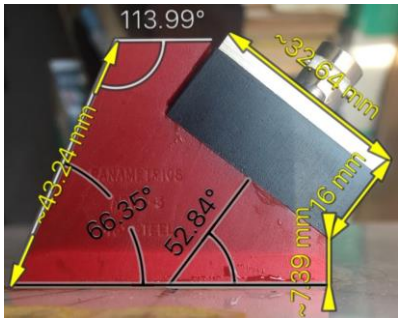

Figure 3. The linear and angular outer dimensions of the used wedge actuator [41]

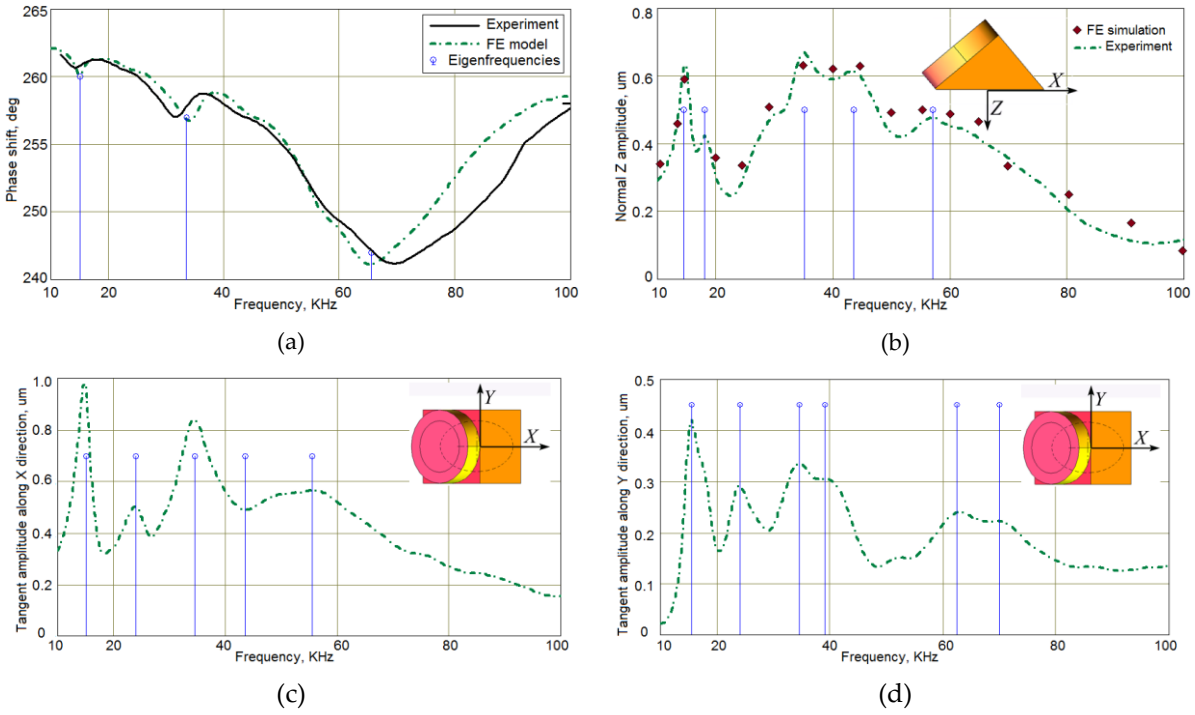

Figure 4. The frequency response functions for the Olympus actuator: (a) - phase angle of PZT current; (b, c, d) - averaged displacement amplitudes on the contact footprint surface - normal (b) and tangential (c, d)

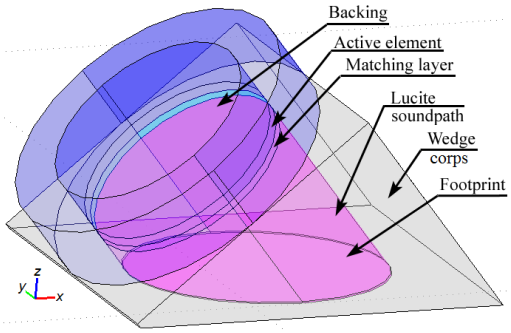

Figure 5. The geometry of wedge actuator's FE model [41]

Preprints (www.preprints.org) | NOT PEER-REVIEWED | Posted: 21 December 2019 doi:10.20944/preprints201912.0279.v1

These results made it possible to obtain preliminary estimates of the waves excitation frequencies, however, these frequencies were subject to refinement due to the interaction of the dynamic system of the actuator and the studied orthotropic CFRP panel.

2.3. Investigation of the wave propagation generated by the oriented angle-beam wedge actuator in orthotropic CFRP panel: Experimental and numerical studies.

Despite the very intensive acoustic waves attenuation, whose angular distribution has been measured by the authors and presented in [19] (see Fig.6), the square CFRP panel was equipped with the porous rubbery absorber to fully eliminate the wave reflections from the edge of the plate (see Fig.7, a). The FE model of the studied system provided this attenuation inside the circle of radius 27.5 cm by the Rayleigh damping coefficients, which depend on the orientation in a polar coordinate system, but outside this circle the damping coefficients increased quadratically while maintaining C^0 and C^1 continuities at the boundary of the circle. By the such way the perfectly matched layer was designed to eliminate the waves reflection. On average, for different frequencies the model consisted of 250-300 thousands of the finite elements; the number of degrees of freedom of the problem is 1.2e6 -1.5e6. The calculation time of one variant with 7-8 fluctuations in the control voltage varied from 4 to 8 hours on a computer with an i7 processor and 32 GB of RAM.

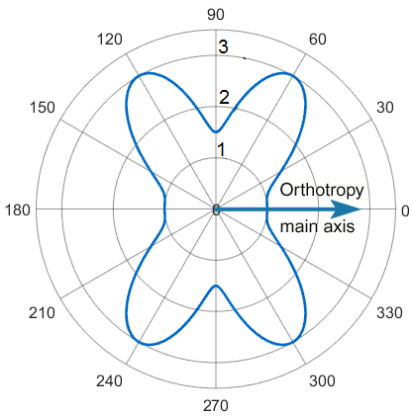

Figure 6. The angular distribution of relative attenuation coefficient for the anti-symmetric A0 waves propagating from the center of the orthotropic CFRP panel [19]

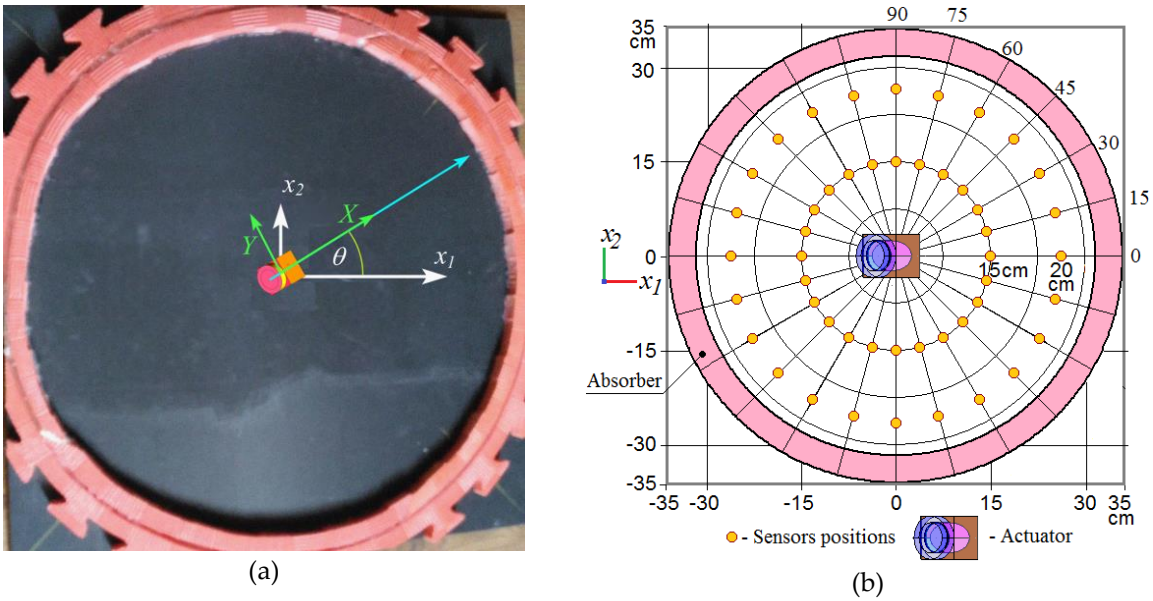

(a) (b)

Figure 7. The experimentally studied CFRP panel with schematically shown coordinate systems of orthotropic symmetry (x_1, x_2) and wedge actuator's (X,Y) rotated relative to the first one by an angle θ (a); the arrangement of sensors for recording the A0 Lamb waves propagation.

Preprints (www.preprints.org) | NOT PEER-REVIEWED | Posted: 21 December 2019 doi:10.20944/preprints201912.0279.v1

In each test, for the variable frequencies and angles of the actuator orientation, the amplitude of the control signal gradually increased, reaching 50 V, and then stabilized (see Fig. 8). These actuator driving signals were prepared using the AWG/AFG software for Windows. They were transmitted to a Tektronix arbitrary function generator and amplified by PA94 piezodrivers (Apex Co., USA). The actuator's and sensors' signals were registered by oscilloscope LeCroy and stored for each testing conditions in the text files, which were then numerically processed.

To exclude possible interference of direct Lamb waves and reflected horizontally polarized SH waves, whose damping is much less, the intensity of the wave A0 detected by the sensors was estimated by averaging the absolute value of the sensors signal during three periods of oscillation, when the signal amplitude stabilizes.

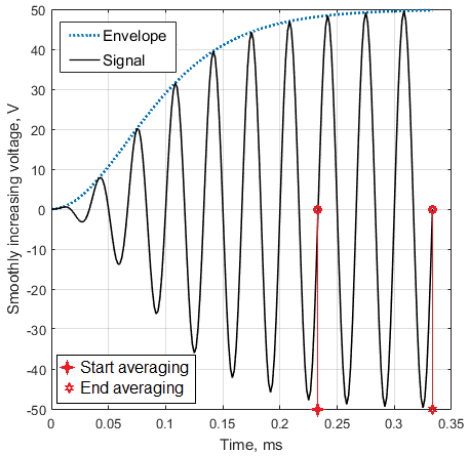

Figure 8. The driving voltage for the PZT actuator and the time interval for the sensor's signal averaging.

The directivity of the waves generated by the wedge actuator has been studied at the three frequencies: 15, 30 and 65 kHz, which were chosen due to the highest intensity of the waves excited at these frequencies. We investigated the directivity of only anti-symmetric Lamb waves A0 because of very long wavelenghts (low spatial resolution) and highly distorted wavefront of the SS0 waves at the used frequencies even at the $\theta=0$ (see Fig.9), which makes the horizontally polarized shear waves unpromising for detection minor defects in high attenuated composites.

The directivity diagrams for the Lamb waves excited by the actuator, whose angular orientation relatively to the main orthotropy axis of the CFRP panel was changed discretely in interval $\theta \in \left[0^0;90^0\right]$ with a step 15^0, was implemented using two identical sensors 15 and 20 cm away from the center of the actuator's footprint (see Fig. 7, b). For each actuator's position these sensor were registered the signals depending on the out-of-plane displacement at their locations. In order to reduce experimental noise the registration of radiation directivity was carried out with an angular step of 15 degrees for two closely spaced distances. Due to attenuation, the signals recorded at distances of 15 cm and 20 cm were unequal. Therefore, the values of both radiation patterns were normalized and averaged. Their values are present in Figs. 10, a - f.

At the numerical simulation, rotation of the actuator direction relative to the main axis of orthotropic anisotropy was carried out by turning its local coordinate system around the axis of the global system, which was normal to the panel plane and passed through its center.

3. Results and Discussion

3.1. Comparison of the experimentally measured and numerically calculated A0 waves directivities.

Some examples of directivity diagrams obtained after the experimental tests and numerical simulations for the different waves excitation frequencies, are presented together in Figures 9, a - f. These plots demonstrate a radical abrupt change in the main orientation of the waves upon rotation

Preprints (www.preprints.org) | NOT PEER-REVIEWED | Posted: 21 December 2019 doi:10.20944/preprints201912.0279.v1

of the actuator, which is confirmed by comparing the calculated data with the experiment. The variability of the waves radiation directivity with frequency is illustrated in Fig. 10, which shows data calculated only by FE model for the entire range of angles of the actuator orientation.

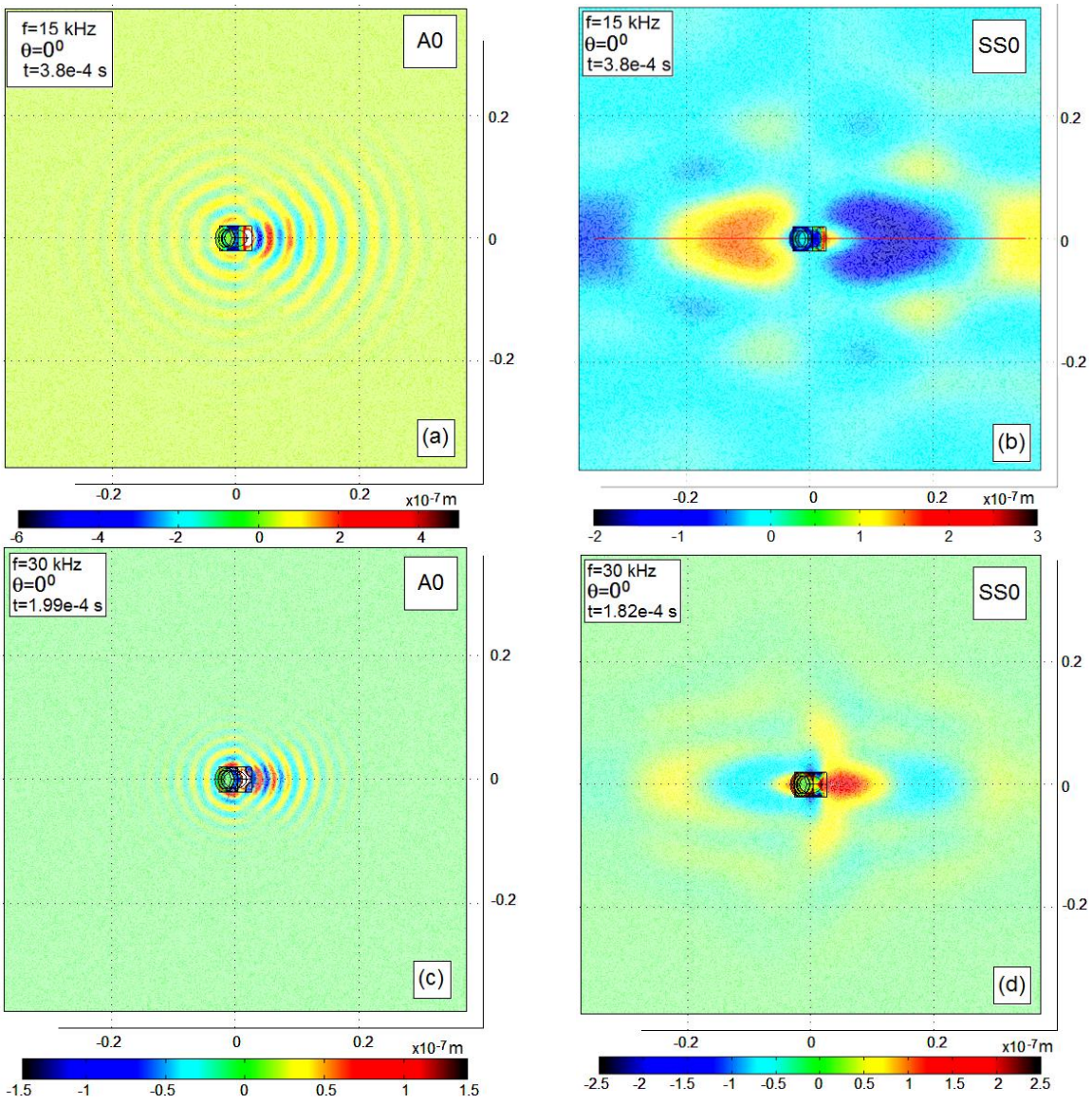

Figure 9. The snapshots of the Lamb (a, c) and SSH (b, d) waves, which propagated in the studied CFRP panel at the frequencies 15 kHz (a, b) and 30 kHz (c, d). Color scales show the normal out-of-plane displacements (a, c) and the radial in-plane displacements (b, d) at the time instants when these displacements have the amplitude values.

These directivity diagrams demonstrate some features that are inherent for highly anisotropic materials. Among these features, which limit the ability of directional waves generation in the composite structures, are:

- wave propagation mainly in the direction of greatest structural stiffness and minimal attenuation;

- deviation of the maximum of the radiation directivity in the direction of the main axis of orthotropic anisotropy, which is confirmed by the fact that when the actuator rotates around an axis perpendicular to the panel surface by a certain angle θ from the main axis, the directivity's lobe rotates by a smaller angle (see Fig. 11);

- the reverse orientation of the wave relative to the orientation of the directional actuator when certain vibration modes are excited in it (see Fig. 11, c).

Preprints (www.preprints.org) | NOT PEER-REVIEWED | Posted: 21 December 2019 doi:10.20944/preprints201912.0279.v1

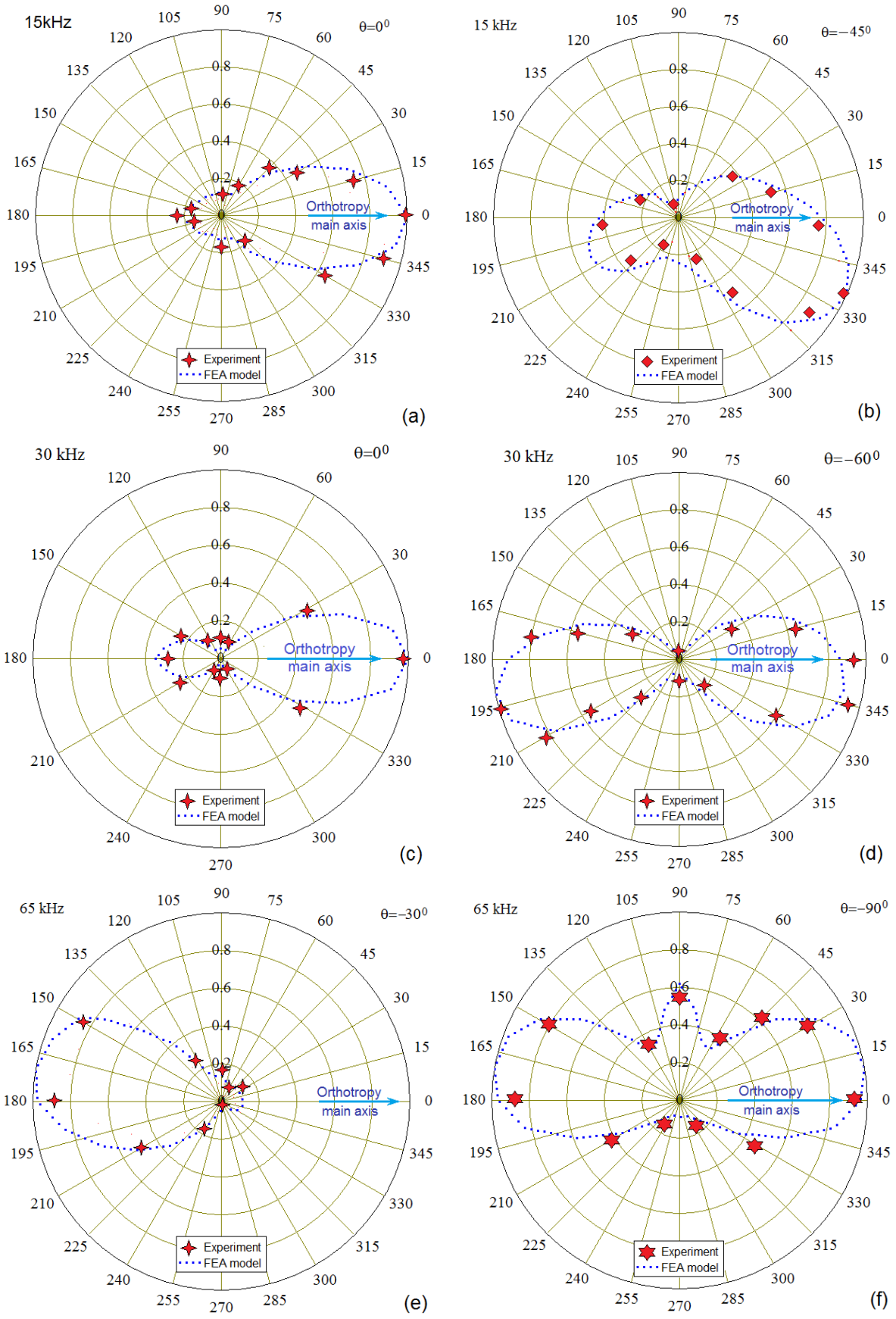

Figure 10. The directivity diagrams of the A0 Lamb waves propagating at the different wedge actuator orientation for the excitation frequencies 15 kHz (a, b), 30 kHz (c, d) and 65 kHz (e, f)

Preprints (www.preprints.org) | NOT PEER-REVIEWED | Posted: 21 December 2019 doi:10.20944/preprints201912.0279.v1

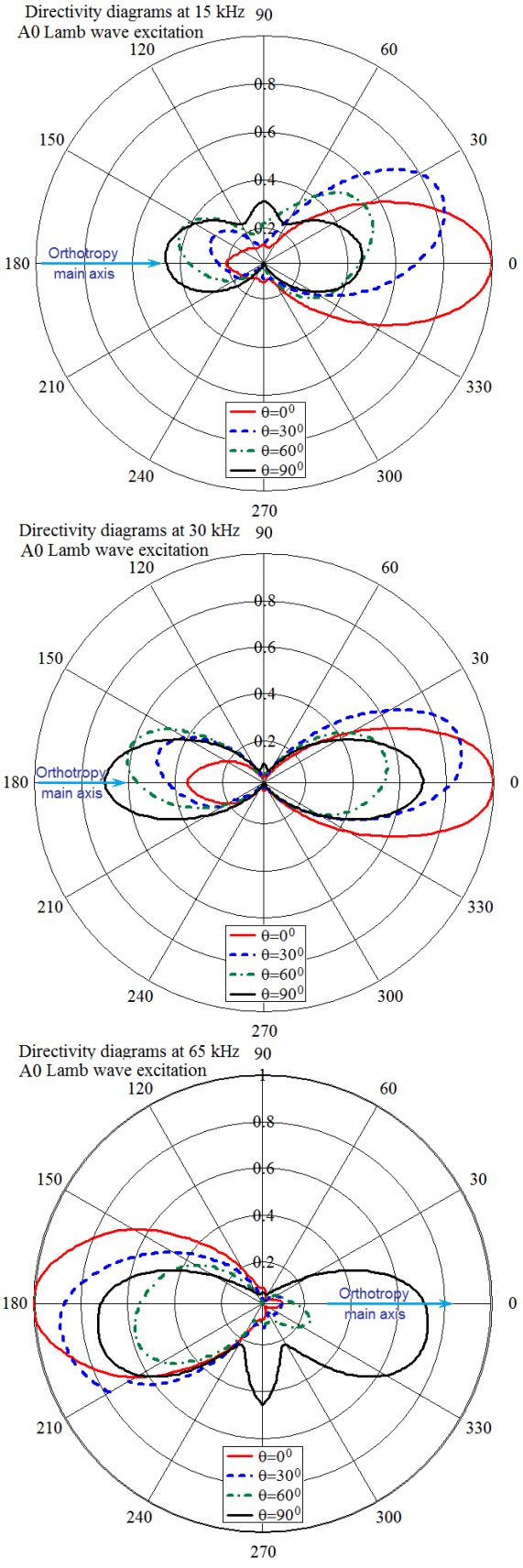

Figure 11. Variation of the A0 Lamb waves directivity with the wedge actuator's angular orientation relative to the main axis of orthotropic symmetry of the CFRP plate at the excitation frequencies 15 kHz (a), 30 kHz (b) and 65 kHz (c)

Preprints (www.preprints.org) | NOT PEER-REVIEWED | Posted: 21 December 2019 doi:10.20944/preprints201912.0279.v1

These features are the result of combination of the actuator's natural modes, shape of its footprint with the anisotropic elastic and damping properties of the thin walled composite structure. All these components determine the stresses on interface between the actuator's footprint and panel's surface, and therefore, the waves propagation.

3.2. Interfacial shear stress and radial tangent displacement distributions: FE simulation results

In order to insights about issues that matter for the wave orientation the postprocessing results of the interfacial stresses and displacements were analyzed at the modeled excitation frequencies. The normal stresses demonstrated irregular plane-like noisy character with small growth when approaching the edges of the footprint, whereas the radial shear stresses amplitudes demonstrated a rather complex, but pronounced spatial distribution corresponding to the natural oscillation modes of the actuator (see Figs. 12).

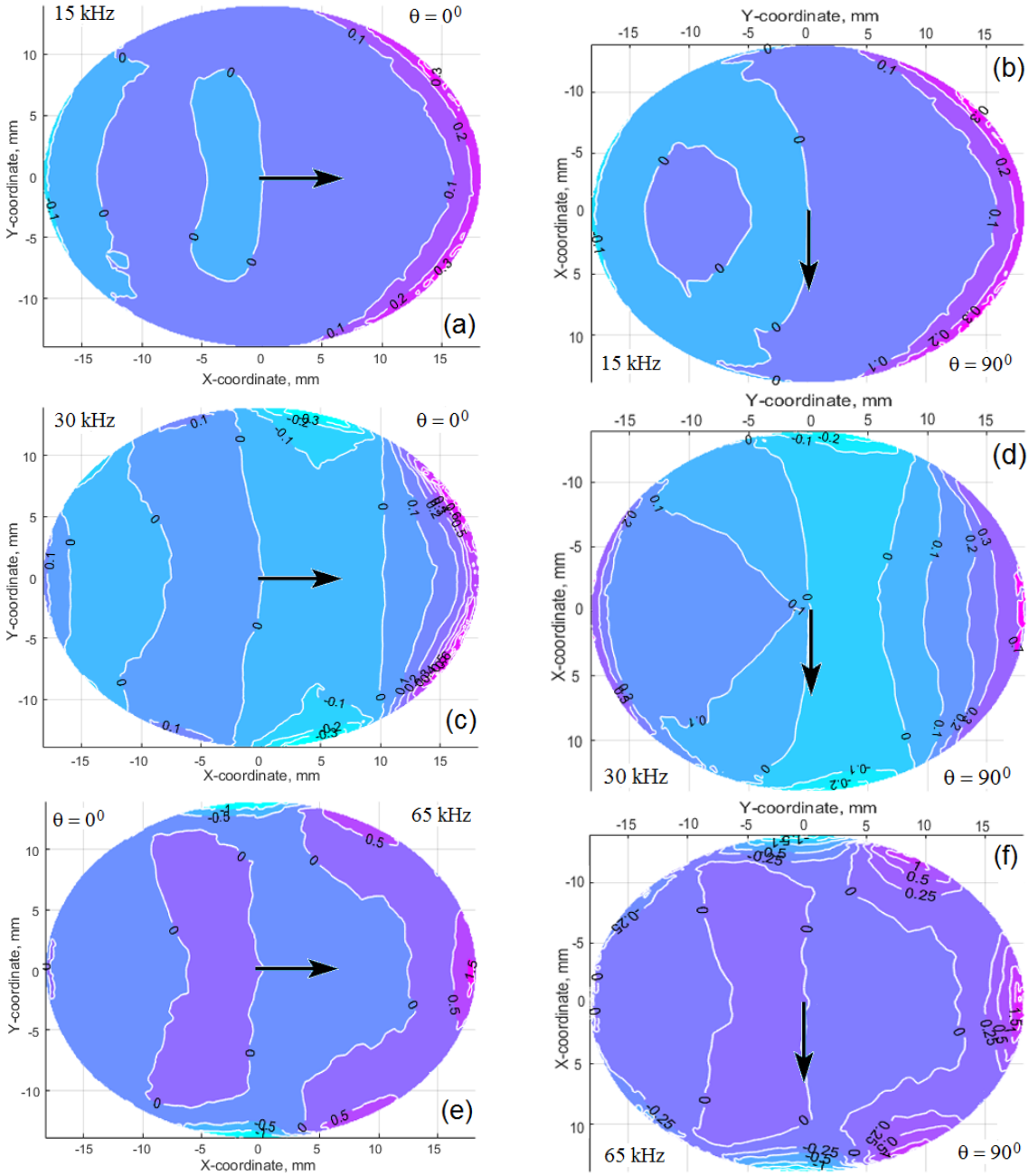

Figure 12. In-plane contact radial stress distributions (amplitude values in MPa) for the waves excitation frequencies 15 kHz (a, b), 30 kHz (c, d) and 65 kHz (e, f) at the actuator orientation along (a, c, e) and across (b, d, f) the main axis of orthotropic panel, which is denoted by the arrows.

Preprints (www.preprints.org) | NOT PEER-REVIEWED | Posted: 21 December 2019 doi:10.20944/preprints201912.0279.v1

Despite the similarity of these tangent radial stress patterns for each excitation frequency (especially at the frequency 65 kHz), the dynamic response of the excited structure depends on the structural and damping anizotropy of the material, and also on the panel thickness, which determine the structural stiffness near the actuator location [20]. Two patterns of the amplitude radial tangent displacements at the same frequency, but at the different actuator orientations: along (a) across (b) the main axis of the orthotropic panel (see Fig. 13), illustrate this statement. As can be seen, the displacements in the direction of greater structural compliance are significantly higher.

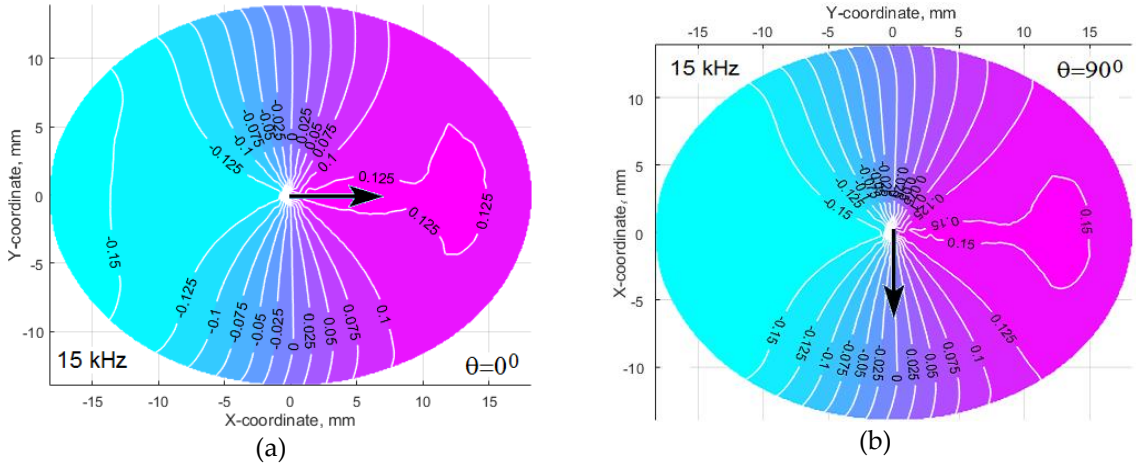

Figure 13. The distribution of the interfacial tangent radial displacements in μm at the excitation frequency 15 kHz. Actuator's axis is oriented along (**a**) and across (**b**) the main orthotropy axis of the CFRP panel, which is denoted by the arrows.

3.3. Attenuation of the Lamb waves generated by the differently oriented wedge actuator

The comparison of two pattern in Figure 13 shows that at $\theta=90^0$ the displacement amplitude in the x_2 direction exceeds the displacement in the x_1, which is explained by the lower stiffness of the material in the x_2 direction. Nevertheless, the directivity diagrams in Fig. 11 demonstrate that the lobe's value along the x_2 direction in is sufficiently less comparing to the lobe's maximum value along x_1 direction. Obviously, it depend on the attenuation of the waves propagating along the directions, which correspond to the maximum of the wave's directivity lobe. The directivity diagrams, which are presented in Fig.11, are averaged for two distances from the actuator. Because the most efficient use of each wave can be reached for the directions, which correspond to the directivity lobe (or lobes), it is very important to estimate the attenuation of the waves propagating along the lobe (or lobes) of maximum intensity. For this purpose the traveling waves amplitudes were calculated for the three distances from the actuator during simulation of all FE developed models for the studied system "CFRP panel - wedge actuator" were investigated. These results are presented in Figure 13. They demonstrate a very high attenuation with the angle θ, especially for the higher frequencies, that can be explained by the anisotropic damping of the studied CFRP composite material and consistent with the results of the works [19 - 27].

All above considered problems, including a correct determination of spatial, frequency and strain type dependent composite material damping, a reasonable choice of the excited acoustic waves taking into account the possibility of their oriented radiation, and the proper choice of the type and dynamic characteristics of the actuator for this purpose are not solved till now with the necessary completeness required for the effective practical use of acoustic-based SHM and NDE of modern composite materials and structures. This is due to the fact that these problems are closely related to each other, and cannot be solved separately. Our analysis of the previous works, which proposed the analytically formulated and solved models, showed that these approaches lose their effectiveness when trying to describe wave phenomena with the necessary accuracy in highly anisotropic composite structures excited by the devices of complex structure and dynamics behavior.

Preprints (www.preprints.org) | NOT PEER-REVIEWED | Posted: 21 December 2019 doi:10.20944/preprints201912.0279.v1

The relatively simple example considered in our article illustrates one of the possible approaches to solving only part of the problem of the rational design such SHM & NDE system.

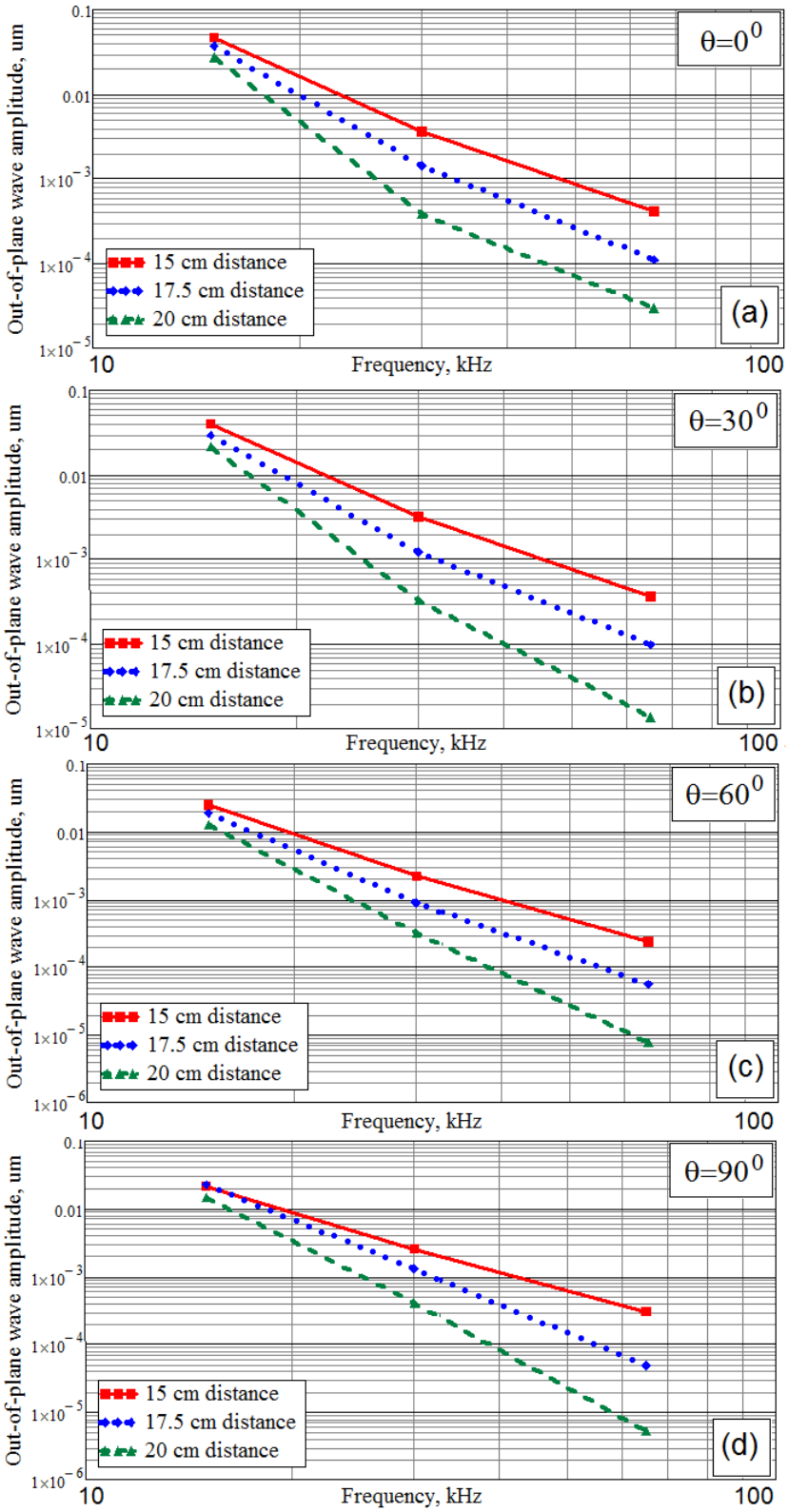

Figure 14. The attenuation of the A0 Lamb waves propagating along the main lobes of the directivity diagrams at the different wedge actuator orientation and the waves excitation frequencies.

4. Conclusions

In this paper we presented some experimental and numerical modeling investigations results of the directed guided-wave excitation by angle-beam wedge piezoelectric actuator in a thin-walled multi-layered composite panel with orthotropic symmetry of the material. Our investigation included the dispersion analysis of the waves that can be excited in the studied panel at the limited frequency range, whose upper limit is caused by the frequency dependent waves attenuation. In order to develop the FE model of the system "CFRP panel - wedge actuator" the dimensional and dynamic properties of the used PZT actuator were identified by comparison the experimental data of its testing and numerical simulation results. For the following detailed analysis the zero order anti-symmetric Lamb wave A0 was chosen because it provide the better spatial resolution for the SHM purpose at the relative low frequencies. For the analysis of the wave directivity, its dependency on the excitation frequency and actuator's orientation relative to the coordinate system of the panel's orthotropic material, only three eigenfrequencies of the wedge actuator were used due to most intense excitation of the waves at these frequencies. As a result of this study, the main regularities of changes in the directivity diagrams of the generated waves were established, as well as the limits of a allowable change in the orientation of the main lobes for an orthotropic material with a variation in the angular orientation of the actuator. For each distinct case of the chosen excitation frequency and actuator's orientation the attenuation of the wave propagating along the main lobe was estimated. The text of the article illustrates the complexity of reasonable decision on the type and frequency of the excited acoustic waves taking into account the anisotropic elastic, damping properties of the material, and the proper choice of the type and dynamic characteristics of the actuator for the SHM purposes. Meanwhile, the relatively simple example, which is considered in this article, illustrates the possible approach to solve these important parts of the problem of the rational design the SHM & NDE systems.

Author Contributions: Conceptualization, E. Kirillova and S. Shevtsov; methodology, S.-H. Chang and S. Shevtsov; experimental investigation, V. Chebanenko and E Rozhkov; software development, M. Shevtsova; FE models development and validation, S. Shevtsov; results numerical processing, V. Chebanenko and M. Shevtsova; writing—original draft preparation, review and editing, S. Shevtsov; supervision and project administration, S.-H. Chang; funding acquisition, S. Shevtsov, S.-H. Chang and E. Kirillova. All authors have read and agree to the published version of the manuscript.

Funding: This research was funded by from the German Federal Ministry of Education and Research (BMBF) (Grant No. 13FH009IX5), Russian Foundation for the Basic Research (Grant No. 16-58-52013), Russian Academy of Science (project A16-116012610052-3), and by Taiwanese Ministry of Science and Technology (Grants MOST107-2221-E-992-027-, MOST 108-2221-E-992-026).

Acknowledgments: The authors wish to acknowledge the valuable technical support from the Institute of Mechanics and Applied Mathematics of the Southern Federal University (Rostov on Don, Russia) directed by professor M. Karyakin provided Acoustic Research Lab for the experimental researches.

Conflicts of Interest: The authors declare no conflict of interest. The funders had no role in the design of the study; in the collection, analyses, or interpretation of data; in the writing of the manuscript, or in the decision to publish the results.

References

1. Kessler, S.S., Spearing, S.M. and Soutis, C. Damage Detection in Composite Materials Using Lamb Wave Methods. *Smart Mater Struct* **2002**, Vol.11, pp.269–278.
2. Kessler, S.S. and Rani, P. Pattern Recognition for Damage Characterization in Composite Materials. *Proceedings of the 48th AIAA/ASME/ASCE/AHS/ASC Structures, Structural Dynamics, and Materials Conference*, (Honolulu, Hawaii, 23 - 26 April 2007; American Institute of Aeronautics and Astronautics), **2007**; 11 p.
3. Sun, Z., Rocha, B., Wu, K.-T., and Mrad, N.A. Methodological Review of Piezoelectric Based Acoustic Wave Generation and Detection Techniques for Structural Health Monitoring. *International Journal of Aerospace Engineering* **2013**, Vol. 2013, 22 p.

4. Andreades, C., Malfense, G.P., Meo, M., Ciampa, F. Nonlinear ultrasonic inspection of smart carbon fibre reinforced plastic composites with embedded piezoelectric lead zirconate titanate transducers for space applications. *J Intel Mat Syst Str* **2019**, Vol. 30 (20), pp. 2995–3007.
5. Gao, Y., Li, Y., Zhang, H., He, X. Modeling of the Damping Properties of Unidirectional Carbon Fibre Composites. *Polymers & Polymer Composites* **2011**, Vol. 19(2 & 3), pp. 119-122.
6. Stepinski, T., Manka, M. and Martowicz, A. Interdigital Lamb Wave Transducers for Applications in Structural Health Monitoring. *NDT&E Int* **2017**, Vol.86, pp. 199-210.
7. Saravanos, D.A., Chamis, C.C. Computational Simulation of Damping in Composite Structures. *NASA Tech.Report* **1989** (Lewis Research Center, Cleveland, Ohio), 27 p.
8. Ono, K., Galego, A. Attenuation of Lamb Waves in CFRP Plates. *J Acoustic Emission* **2012**, Vol.30, pp. 109-123.
9. Ramadas, C. Three-Dimensional Modeling of Lamb Wave Attenuation Due to Material and Geometry in Composite Laminates. *J Reinf Plast Comp* **2014**, Vol. 33, pp. 824-835.
10. Gresil, M., Giurgiutiu, V. Prediction of Attenuated Guided Waves Propagation in Carbon Fiber Composites Using Rayleigh Damping Model. *J Intel Mat Syst Str* **2015**. Vol. 26(16), pp. 2151-2169.
11. Hu, N., Liu, Y., Peng, X. and Yan, B. Optimal Excitation Frequency of Lamb Waves for Delamination Detection in CFRP Laminates. *J Compos Mater* **2010**, Vol. 44, pp. 1643-1662.
12. Han, K. and Lee, L.J. Dry Spot Formation and Changes in Liquid Composite Molding: I-Experimental. *J Compos Mater* **1996**, Vol 30 (13), pp. 1458-1474.
13. Bertling, B., Kaps, R. and Mulugeta, E. Analysis of dry-spot behavior in the pressure field of a liquid composite molding process. *CEAS Aeronaut J* **2016**, Vol. 7, pp.577-585.
14. Im, K.-H., Kim, H.-J., Song, S.-J., Hsu, D.K., Lee, K.-S., Yang, I.-Y., and Park J.-W. Feasibility on Generation mechanism of Ultrasonic Shear Wave for the Application on Stacking Orientation Defect in CFRP Composite Laminates. *AIP Conf Proc* **2009**, Vol.1096, pp.1033-1040.
15. Giurgiutiu, V. Tuned Lamb Wave Excitation and Detection with Piezoelectric Wafer Active Sensors for Structural Health Monitoring. *J Intel Mat Syst Str* **2005**, Vol. 16, pp.291-305.
16. Raghavan, A. and Cesnik, C.E.S. Modeling of Guided-Wave Excitation by Finite-dimensional Piezoelectric Transducers in Composite Plates. *Proceedings of the 48th AIAA/ASME/ASCE/AHS/ASC Structures, Structural Dynamics, and Materials Conference*, (Honolulu, Hawaii, 23 - 26 April 2007; American Institute of Aeronautics and Astronautics), **2007**; 15 p.
17. Schultz, A.B. and Tsai, S.W., Measurement of Complex Dynamic Moduli for Laminated Fiber Reinforced Composites. *J Compos Mater* **1969**, Vol. 3, pp. 434- 444.
18. Watanabe, Y., Biwa, S. and Ohno, N. Experimental Investigation of Ultrasonic Attenuation Behavior in Carbon Fiber Reinforced Epoxy Composites. *J Soc Mat Sci*, (Japan) **2002**, Vol.51(4), pp. 451-457.
19. Shevtsova, M. et al. Piezoelectric Based Lamb Waves Generation and Propagation in Orthotropic CFRP Plates: I. Influence of Material Damping. *Mater Sci Forum* **2019**, Vol. 962, pp. 218-226.
20. Shevtsova, M. et al. Piezoelectric Based Lamb Waves Generation and Propagation in Orthotropic CFRP Plates: II. Influence of Interfacial Stress Distribution. *Mater Sci Forum* **2019**, Vol. 962, pp. 227-235.
21. Chinchan, L. et al. Mechanical Testing of Polymeric Composites for Aircraft Applications: Standards, Requirements and Limitations. In *Advanced Materials. Springer Proceedings in Physics;* Springer ed., Berlin, Heidelberg, New York, **2014**, Vol. 152, pp.201-221.
22. Kamal A.M., Taha I. Vibration Damping Behavior of Fiber Reinforced Composites: A Review. *Key Eng Mater* **2010**, Vol. 425, pp. 179-194.

23. Adams, R.D., Fox, M.A.O., Flood, R.J.L. and Hewitt, R.J. The Dynamic Properties of Unidirectional Carbon and Glass Fiber Reinforced Plastics in Torsion and Flexure. *J Compos Mater* **1969**, Vol. 3, pp. 594-603.
24. Crane, R.M. Vibration Damping Response of Composite Materials. *David Taylor Research Center Report* **1991**, 302 p.
25. Hashin, Z. Complex moduli of viscoelastic composites—I. General theory and application to particulate composites. *Int J Solid Struct* **1970**. Vol. 6 (5), pp. 539-552.
26. Vojiadjis, G.Z. and Kattan, P.I., *Mechanics of Composite Materials with MATLAB*; Springer, Berlin, Hedelberg, 2005, 336 p.
27. Adams, M.R. and Maheri, M.R. Dynamic Flexural Properties of Anisotropic Fibrous Composite Beams. *Compos Sci Technol* **1994**, Vol.50, pp. 497-514.
28. Kim I. and Chattopadhyay A. Guided Lamb Wave–Based Structural Health Monitoring Using a Novel Wave Packet Tracing Method for Damage Localization and Size Quantification. *J Intel Mat Syst Str* **2015**, Vol. 26 (8), pp. 2515-2530.
29. Ostiguy, P.-C., Quaegebeur, N ., Bilodeau, M. and Masson, P. Semi-Analytical Modelling of Guided Waves Generation on Composite Structures Using Circular Piezoceramics. *Proc. SPIE* **2015**, Vol. 9438, Health Monitoring of Structural and Biological Systems 2015, 14 p.
30. Su, Z., Ye, L. Selective Generation of Lamb Wave Modes and their Propagation Characteristics in Defective Composite Laminates. *Proc Inst Mech Engrs* **2004**, Vol. 218, pp.95-110.
31. Viktorov, L.A., *Rayleigh and Lamb Waves: Physical Theory and Applications;* Plenum, New York, 1967, 160 p.
32. Bertoni, H. L. Design Considerations for Efficient Wedge Transducers. *Proceedings of the 3rd European Microwave Conference*, **1973** (Brussels, Belgium, 4-7 Sept. 1973; European Microwave Association), 4 p.
33. Alphonse, G.A. The Wedged Transducer — A Transducer Design for Broad Band Characteristics. *Ultrasonic Imaging* **1979**,Vol.1(1), pp. 76–88.
34. Ditri, J.J. and Rajana, K.M. Analysis of the Wedge Method of Generating Guided Waves. *Review of Progress in Quantitative Nondestructive Evaluation* **1995**, Vol. 14, pp. 163-170.
35. Rus, G., Wooh, S.-C. and Gallego R. Analysis and Design of Wedge Transducers Using the Boundary Element Method. *J Acoust Soc Am* **2004**, Vol. 115 (6), pp.2919-2927.
36. Jin, D. and Li, Z. Simulation and Optimization of Wedge-Shaped Ultrasonic Transducers Using Finite Element Method (FEM). *Appl Mech Mater* **2013**, Vol. 281, pp.112-115.
37. Zhao, X., Schmerr L.W., Jr., Sedov, A., and Li, X. Ultrasonic Beam Models for Angle Beam Surface Wave Transducers. *Res Nondestruct Eval* **2016**, Vol. 27 (3), pp. 175-191.
38. Zhang, S., Li, X., Jeong, H. and Hu H. Modeling nonlinear Rayleigh wave fields generated by angle beam wedge transducers—A theoretical study. *Wave Motion* **2016**, Vol. 67, pp. 141–159.
39. Zhang, S., Li, X., Jeong, H. and Hu, H. Modeling Linear Rayleigh Wave Sound Fields Generated by Angle Beam Wedge Transducers. *AIP Adv* **2017,** Vol. 7, pp.015005-1 - 13.
40. Zhang, S., Li, X., and Jeong, H. Measurement of Rayleigh Wave Beams Using Angle Beam Wedge Transducers as the Transmitter and Receiver with Consideration of Beam Spreading. *Sensors* **2017**, Vol.17(6), 18 p.
41. Shevtsov, S., Chebanenko, V., Shevtsova, M., Kirillova, E., and Rozhkov, E. On the Directivity of Acoustic Waves Generated by the Angle Beam Wedge Actuator in Thin-Walled Structures. *Actuators* **2019**, Vol. 8(3), 64, pp. 16.
42. Barbero, E.J. *Finite Element Analysis of Composite Materials with Abaqus*; CRC Press, Boca Raton, London, New York, **2013**, 406 p.

 doi:10.20944/preprints201912.0279.v1

43. Rose, J.L. *Ultrasonic guided waves in solid media*; Cambridge University Press, New York, **2014**; 547 p.
44. Olympus NDT Instruments. Available online: URL Olympus-ims.com/en/ndt-instruments.